Chemistry–A European Journal
Research Article
doi.org/10.1002/chem.202201446
Chemistry Europe
European Chemical Societies Publishing
www.chemeurj.org

Reversible Photoinduced Conversion of Unprecedented Norbornadiene-Based Photoswitches with Redox-Active Naphthalene Diimide Functionalities

Andreas Leng[+],[a] Cornelius Weiß[+],[a] Nina Straßner,[a] and Andreas Hirsch*[a]

Abstract: An unprecedented compound class of functional organic hybrids consisting of a photoswitchable norbornadiene building block and a redoxactive chromophore, namely naphthalene diimide, were designed and synthesized. Within these structures the capability of rylene chromophores to function as a redox active catalyst upon their photoexcitation was utilized to initiate the oxidative back-conversion of the in situ formed quadricyclane unit to its norbornadiene analogue. In this way successive photoexcitation at two different wavelengths enabled a controlled photoswitching between the two isomerical states of the hybrids. Beyond this prove of concept, the dependency of the reaction rate to the intramolecular distance of the two functional molecular building blocks as well as the concentration of the photoexcited sample was monitored. The experimental findings and interpretations were furthermore supported by quantum chemical investigations.

Introduction

As a consequence of the aggravating climate change and the urgent need to reduce greenhouse gas emission caused by fossil fuels, research into sustainable energy conversion and storage has been constantly growing.[1] This also applies to the molecular solar thermal (MOST) system consisting of the isomeric couple norbornadiene (NBD) and quadricyclane (QC), which has been continuously investigated and optimized towards practical applicability since the late 1960's.[2] A tailored storage system of this type can be implemented in a multitude of applications, such as pre-heating of various industrial processes, domestic heating and even electricity generation.[2b,3] During the potential storing process, the photochromic compound NBD can undergo a reversible light-induced valence isomerization to its metastable analogue QC. Since parent NBD shows no significant absorption above 226 nm, the rearrangement is not triggered by visible sunlight or conventional light sources.[4] This insensitivity of NBD towards a large part of the solar spectrum can be overcome by the use of appropriate triplet sensitizers or by the functionalization and modification of the NBD skeleton itself. Especially 2,3-disubstituted derivatives in which one double bond is incorporated into a conjugated push-pull system were found to have a bathochromically shifted absorption.[5] During the light-induced isomerization energy (-89.03 ± 1.10 kJ/mol) is stored in the highly strained carbon framework of quadricyclane (QC).[6] Despite its unfavorable structure QC is kinetically quite stable since the back-conversion to norbornadiene is a concerted $_{\pi}2\,s + _{\pi}2\,s$ ring opening, which is formally forbidden by the Woodward-Hoffmann rules.[7] The energy barrier of 140 kJ/mol caused by these orbital restrictions prevents a spontaneous back-conversion to NBD.[8] This can be achieved either by metal-ligand orbital interactions in the presence of specific transition metal complexes, or by the oxidation of QC.[9] Both pathways of controlled energy release have been utilized in previously published work of our group.[10] Within these projects a magnetic supramolecular catalyst, suitable for macroscopic heat release from various storage couples, was developed by the immobilization of tailored transition metal complexes on Fe_3O_4 nanoparticles.[10b] The different anchored Co(II)-complexes captivate by their high catalytic activity, their robustness and a straightforward separation by an external magnetic field. By combining them with various interconversion couples, an adjustable process for molecular solar thermal energy storage was developed.[11] In addition to this work, the lowered energy barrier of 40 kJ/mol for the oxidized species $QC^{\bullet+}$, bearing the potential for a rapid back-conversion to NBD, motivated us to exploit this reaction mechanism (see Scheme 1) to develop metal-free catalysts and NBD/QC-based photoswitches.[8b,12] With a comparatively low oxidation potential of $+0.91$ V (vs. S.C.E) QC is readily oxidized to $QC^{\bullet+}$.[13] This cationic species, which was monitored by CIDNP and TP-ESR measurements, was found to rapidly rearrange to its corresponding NBD isomer.[14] This redox-initiated ring opening can even be induced by quenching the photoexcited singlet state of organic electron acceptor sensitizers. A variety of aromatic hydrocarbons have

[a] A. Leng,[+] C. Weiß,[+] N. Straßner, Prof. Dr. A. Hirsch
Department of Chemistry and Pharmacy
Friedrich-Alexander-Universität Erlangen-Nürnberg
Nikolaus-Fiebiger-Str. 10, 91058 Erlangen (Germany)
E-mail: andreas.hirsch@fau.de
[+] These authors contributed equally to this work.

Supporting information for this article is available on the WWW under https://doi.org/10.1002/chem.202201446

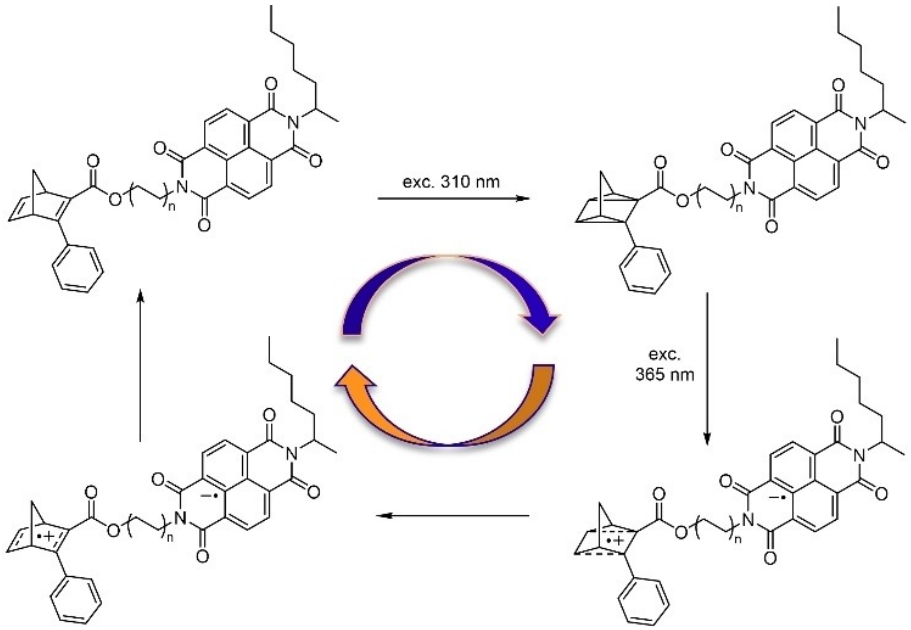

Scheme 1. Schematic depiction of the photoconversion of unprecedented NBD-NDI-hybrid structures to their corresponding QC analogue including the proposed transition states.

been reported to oxidize QC upon the quenching of their photoexcited singlet state and therefore initiate the isomerization to NBD.[15] In one of our previously reported projects the electron acceptor C_{60} was linked to NBD.[10a] These hybrid architectures can be repeatedly photo-switched between the NBD and QC state upon the photoexcitation of either one of the functional building blocks. Driven by the success of this work, we conducted preliminary experiments in which we tested additional electron-deficient aromatic chromophores to photo-induce this interconversion. These results and previous reports on their photo-oxidative activity, demonstrated the suitability of naphthalene bisimides, a compound class of redox active chromophores, to cause a rapid rearrangement of QC upon quenching of their photoexcited state.[16] These smallest representatives of the rylene dyes have suitable properties with respect to thermal and chemical stability, absorption properties and are characterized by a strong electron affinity with a redox potential of −1.10 V (vs. Fe/Fe^{+}).[17] Naphthalene bisimides have been reported to readily act as photoactive redoxcatalysts.[18] Due to their high electron affinity, they can undergo a photo-induced electron transfer in the presence of suitable organic electron donors, causing the oxidation of the latter.[19] The pathway of this light-induced redox reactions, which match the requirements on a photocatalytic pathway for the QC/NBD interconversion, can be confirmed by the spectroscopical monitoring of the formed NDI radical anion.[20] Based on these reported findings we concluded that NDIs have the potential to serve as a metal-free redox-active photocatalyst for various NBD/QC interconversion couples. In addition to that, their implementation in a molecular norbornadiene-based architecture would lead to the formation of compounds which can be reversibly switched between two isomeric states when stimulated with light of different wavelengths.[10a] The resulting photoswitches can therefore not only be applied in energy harvesting, their ability to be reversibly switched between different states also enables their implementation in optoelectronic devices as OFETs, organic photodiodes or molecular logic systems.[21] We have now developed unprecedented, covalently-linked hybrid structures consisting of a switchable NBD/QC building block and a naphthalene bisimide dye and investigated their photoswitching properties. The implemented NBD derivative is a 2,3-disubstituted push-pull derivative whose absorption maximum is bathochromically shifted to 293 nm. This enabled us to carry out the light-induced isomerization employing a customized photoreactor equipped with UV-LEDs. Apart from its suitable absorption behavior the incorporated NBD derivative **2** (see Scheme 2) is known for the thermal stability of its QC analogue and the embedded carboxyl group facilitates subsequent chemical modification.[10b,22] In this position the derivative was linked to a naphthalene bisimide via three different alkyl spacers with varying length. Not only was a viable procedure developed to efficiently synthesize NBD-NDI hybrid structures, the three reported structures were also investigated with respect to their photo-induced interconvertibility. A subsequent excitation of the NBD feature followed by an irradiation in the range of the NDI's absorption maximum resulted in a repeatable cyclization of both isomeric states. The observed rapid back-conversion of QC to NBD upon the quenching of the photo-excited NDIs clearly demonstrates their tremendous potential as photo-oxidative catalysts. Not only was the impact of a varying intramolecular distance on the reaction rate of both interconversions monitored, but also the influence of differing concentrations was scrutinized. In addition to our practical work, we report a detailed quantum mechanical

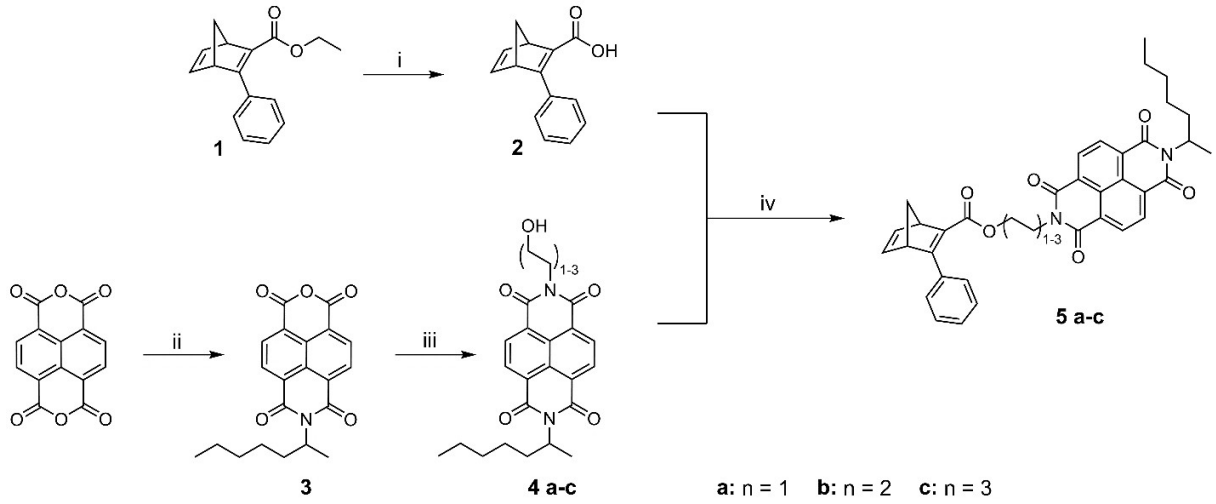

Scheme 2. Synthesis of the NBD-NDI-hybrids with varying length of their alkyl spacer. The conditions and reagents applied in the consecutive reaction steps were the following: i) NaOH, H_2O/THF, 70 °C, 7 d; ii) 2-heptylamine, AcOH, DMF, reflux, 1.5 h; iii) 2-amino-ethanol (**4a**), 4-amino-butanol (**4b**), 6-amino-hexanol (**4c**), DMF, 130 °C, 1.5 h; iv) DCC, DMAP, DCM, reflux, 4–6 h.

investigation of particular target molecules and individual building blocks.

Results and Discussion

Synthesis of NBD-NDI-hybrid architectures

Our synthesis was aimed at molecular architectures combining two functional building blocks, namely an NBD unit with optimized absorption features and a naphthalene bisimide chromophore (NDI). Both molecular frameworks were planned to be linked via the NDI's *imide*-position by alkyl chains of varying length. Despite their high flexibility, we were expecting the variation of the intramolecular distance of both building blocks to impact the reaction rate of the photo-oxidative back-conversion of QC to NBD. The *imide*-position is a comparatively easily addressable functionality to which the spacers could be attached without affecting the absorption features of the NDI itself. We decided to choose the 2,3-disubstituted push-pull NBD **1** as a precursor. This compound, which features a bathochromically shifted absorption and a decent chemical und thermal robustness, was well-known in our working group and has been used in previous experiments as a model system.[10a] The two functional building blocks, NBD and NDI, were planned to be linked in a final reaction step via a Steglich esterification.[10a,23] By a saponification in the presence of NaOH, compound **1** was transformed into the carboxylic acid **2** which served as a precursor for the subsequent reaction step, the Steglich esterification. The two-step synthesis of the second required precursor, the hydroxylated NDI (**4**), is depicted in Scheme 2. The first reaction was a condensation between NTCDA and 2-aminoheptane in acidic media forming naphthalene monoamide (NMI) **3**. Although the nucleophilic character of the amine is diminished by protonation, the anhydride functionality is activated which is beneficial for the outcome of the reaction. The introduced asymmetric alkyl chain, which was found to result in higher yields then symmetrical ones, provides the required solubility of the target molecule. The steric demand of the residue inhibits the distinctive intermolecular π-π-stacking which prevents the molecules to agglomerate and precipitate from solution. The comparatively low yield of this reaction can be attributed to the additional formation of the symmetrical NDI in which both anhydride functionalities of the precursor are transformed to imides. Despite this drawback the reaction was in our case still more effective than the alternative route which includes multiple steps such as an esterification of the anhydride functionality to yield the target NMI.[24] In the next reaction step NMI **3** was converted into the hydroxylated NDIs **4a–c** using similar reaction conditions as described for the previous step. In three separate experiments compound **3** was brought to reaction with different alkanolamines with varying chain lengths. The reaction products were linked to the NBD precursor **2** via a Steglich esterification in which we observed an exceptional increase of the yield when deploying an excess of NBD **2** and increased amounts of DCC and DMAP. The structure and purity of all three target molecules **5a–c** was proven by state-of-the-art characterization including ^{1}H NMR spectroscopy. The recorded spectrum of NBD-NDI **5a** is exemplarily depicted in Figure 1 and the assignment of all signals can be deduced from the color coding.

The absorption properties of all NBD-NDI hybrids and their corresponding precursors **2** and **4a** were determined by UV/Vis spectroscopy. The spectra were recorded in dichloromethane (DCM) and are depicted in Figure 2. All NDIs show similar absorption patterns which are mainly defined by three prominent bands with increasing intensity at 340, 360 and 380 nm. These bands can be attributed to the three electronic transitions from the vibrational energy level $v=0$ of the

Research Article
doi.org/10.1002/chem.202201446

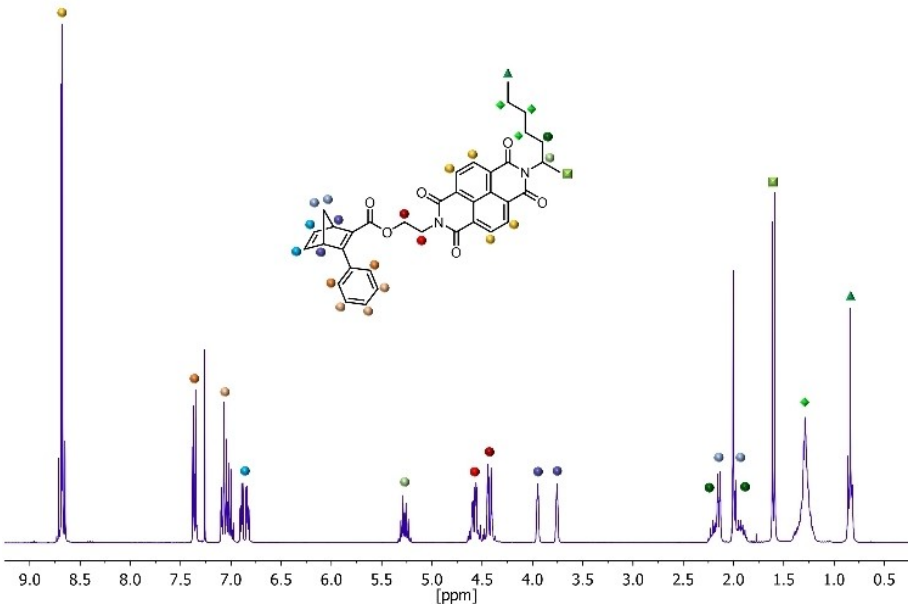

Figure 1. The ^{1}H NMR spectrum of compound **5 a** recorded at 400 MHz in $CDCl_3$. The color coding is intended to facilitate the assignment of the signals to the corresponding protons.

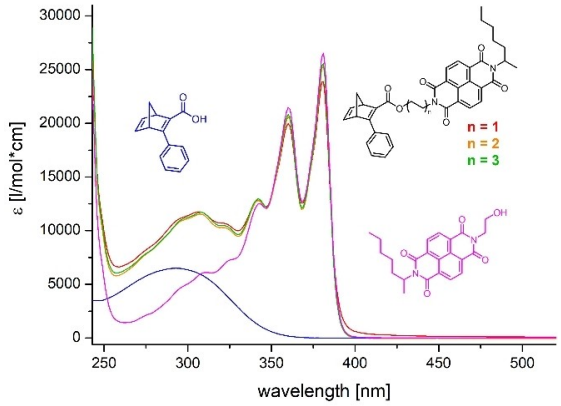

Figure 2. UV/Vis absorption spectra of the relevant precursors **2** and **4 a** and all three synthesized NDI-NDI-hybrids **5 a**–**c** recorded in DCM.

electronic ground state S_0 to $v = 1$ of the three excited states S_1, S_2 and S_3 and are highly characteristic for NDI derivatives. The NBD precursor **2** is characterized by a broad absorption band with a maximum at 293 nm. This feature also seems to increase the extinction coefficient of the NBD-NDI hybrids **5 a**–**c** in the range of 260 to 330 nm in comparison to the non-functional NDI precursor **4 a**.

Photoswitching experiments

The three NBD-NDI-hybrids **5 a**–**c** were systematically analyzed regarding their photoisomerization behavior (see Scheme 3). The experimental setup consisted of three NMR tubes which were equipped with a 15.9 mM solution of each NBD-NDI-hybrid **5 a**–**c** in toluene-d_8, respectively. Previous studies,

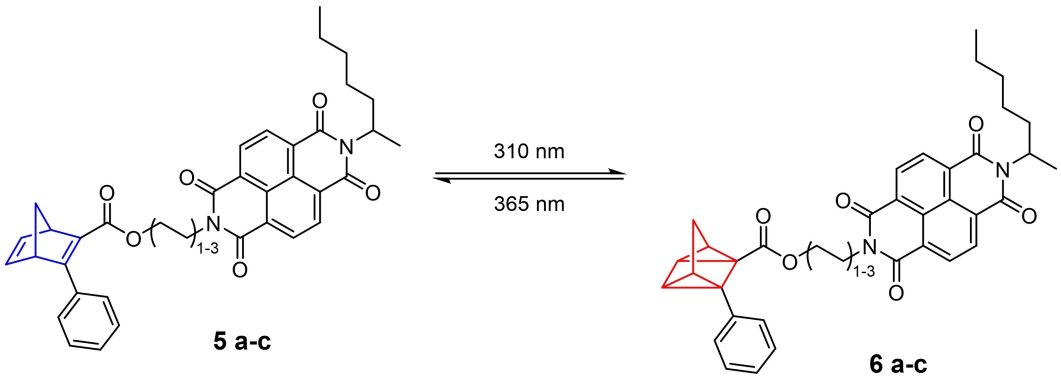

Scheme 3. Schematic depiction of the performed photoexperiments with compound **5 a**–**c** in toluene-d_8.

performed in our working group, indicated that toluene was the most suitable solvent with respect to side-reactions, reaction rate and solubility.[11] All three NBD-NDI hybrids were irradiated with an UV-LED emitting at 310 nm in a custom-build photoreactor. The photoinduced isomerization of the NBD hybrids to their corresponding QC analogues was monitored by periodic ^{1}H NMR measurements. The progress of this rearrangement was defined by the ratio of both isomers based on the integrals of characteristic NMR signals such as the multiplet at 6.91–6.82 ppm, caused by the olefinic protons of the NBD building block. The lack of unattributable NMR-signals and the constant sum of integrals of NBD and QC signals show that no unwanted side-reactions are occurring during the isomerization. After 60 min of continuous photoexcitation at 310 nm a photostationary point was reached and the rearrangement conversion plateaued at 15.5 %–16.5 % of the converted QC-NDI hybrids for all three derivatives. At this point the irradiation was stopped. Based on the data plotted in Figure 3, no decisive difference with respect to the conversion dynamics could be observed for the three compounds **5 a**–**c** during the light-induced isomerization to their QC analogue. A viable explanation for this phenomenon is based on the partial overlap of the absorption features of the NBD and the NDI building blocks. A concurrent photoexcitation of the NDI during the irradiation at 310 nm can cause a parallel photo-oxidative back-conversion to NBD, resulting in an equilibrium of both isomeric states. To initiate the photocatalyzed back-isomerization all three samples were subsequently irradiated at 365 nm while the reaction progress was again monitored by ^{1}H NMR spectroscopy. During this photo-induced process a correlation between the length of the alkyl linker and the reaction rate became apparent (see Figure 3). The data clearly shows that an elongation of the linker between the QC and the NDI building blocks causes an increased back-reaction rate. While the QC derivative of compound **5 c** was fully transformed to its NBD analogue in less than 20 min of excitation, the ethano-linked compound **5 a** was not fully regained even after 50 min. This unequivocal trend in the reaction rate based on the length of the linker in three samples of the same concentration gives rise to the assumption that the underlying mechanism is an intramolecular process. An increased chain length could facilitate π-π-interactions present in less strained conformers between the phenyl substituent and the NDIs aromatic core and therefore accelerate the oxidative back-conversion. To further support this hypothesis and to preclude a catalytic pathway via an intermolecular process, we conducted similar experiments in which three samples of compound **5 b** with varying concentrations were photo-excited. After irradiating all three samples at 310 nm for 60 min, the excitation wavelength was again switched to 365 nm to initiate the back-conversion of the formed QC-NDI-hybrid to compound **5 b**. The results from these experiments, which are plotted in Figure 4, show a decreasing reaction rate for both isomerization steps with increasing concentration of the irradiated sample. In case of the back-conversion of the QC species to NBD-NDI **5 b** upon irradiation at 365 nm, this trend becomes even more apparent once the measured concentrations of QC-NDI were normalized (see Figure 5). Previous studies on NBD systems revealed a direct correlation between increasing concentrations and rising quantum yields of the investigated samples.[11]

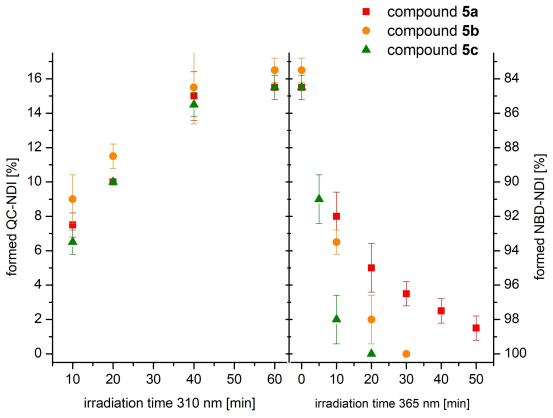

Figure 3. Conversion rates of compounds **5 a**–**c** upon the photoexcitation at 310 nm and subsequent excitation at 365 nm. During the isomerization to the QC derivatives no clear correlation between the reaction rate and the spacer length could be observed. The back-conversion proceeded faster with increasing spacer length.

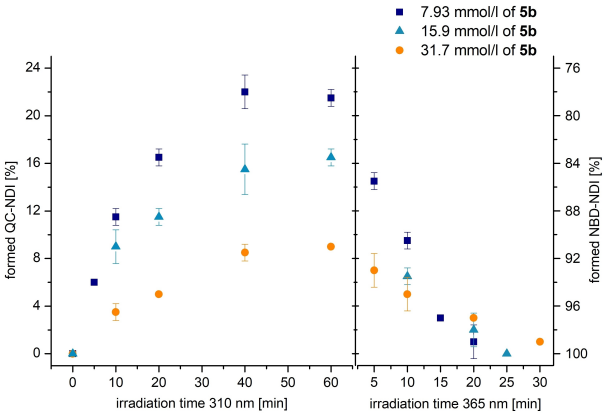

Figure 4. Monitoring the reaction rate of both isomerization steps of compound **5 b** in correlation with a varying concentration of the irradiated sample revealed a dependency of concentration and rate of isomerization.

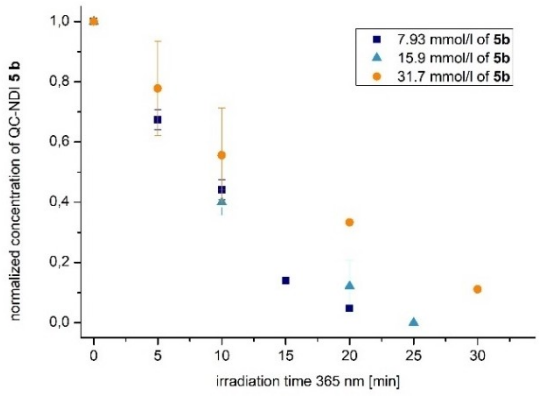

Figure 5. Normalized concentration of formed QC derivatives as a function of the irradiation time (365 nm).

Contrary to these results, we observed a decrease of reaction rate with increasing concentration. A possible explanation for this opposed effect is the increase in collisional quenching within samples of higher concentration. In this way the photocatalytic potential of the NDI building block is diminished by the collision with other NDI species which function as a quencher. Although it seems to be the most viable theory, further experimental proof needs to be obtained to legitimate this assumption.

Computational investigations

The unsubstituted couple NBD and QC has previously been studied by computational methods. These revealed *inter alia* the relative energy levels of the photoisomerization, the thermal back-conversion and of all included radical cations and transition states in 1996.[25] These calculations which were carried out by Bach et al. are based on the MP4/6-31G*//MP2/6-31G* level of theory, which was state of the art at this point of time. Since it is known to be a reliable combination of functional and basis set for this type of molecules, we decided to use B3LYP/6-311++G* level of theory extended by Grimme's D3 model with Becke-Johnson damping functions to take dispersion interactions into account.

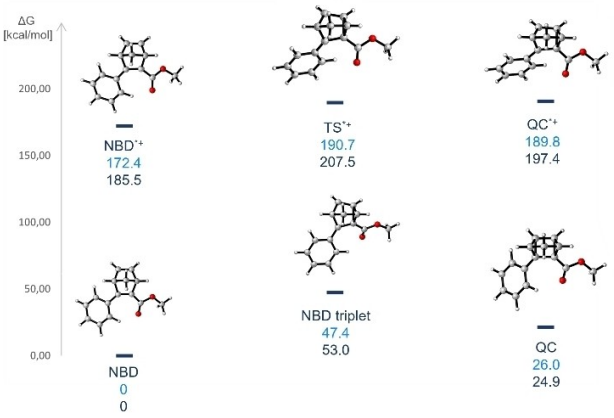

Figure 6. Relative energies of the isomerization of the unsubstituted NBD/QC (dark blue) and the depicted 2,3-disubstituted model compound (light blue) at the B3LYP/6-311++G** level of theory with D3BJ dispersion correction. All energies are given in kcal/mol.

Both, the unsubstituted and a 2,3-disubstituted NBD model compound in which the NDI functionality was replaced by a methyl group, were studied based on this method. The calculated relative energies of all relevant species occurring during both possible mechanistic pathways, the isomerization via a triplet state and through a radical cation transition state, can be found in Figure 6.

The multitude of possible orientations of the phenyl and ester functionalities in the 2,3-disubstituted model compound leads to various conformational isomers. It was necessary to identify the conformer with the lowest relative ground state energy and use this geometry for the determination of the relative energies of transition states and the influence of dispersion interactions. As shown in Figure 7, the ester functionality can have three different orientations relative to the phenyl group, while the substituents are too large to both be in one plane, causing the ester group to either be above or below the ring plane of the phenyl ring. Our calculations have shown that isomer **a** is slightly favored relative to **b** in both the NBD and QC ground states. The energy difference between both states, however, was beneath 1 kcal/mol, which is why not all structures for the isomerization mechanism were calculated. The comparison of the energies of conformers **1** to **3** in the entire mechanism (Table 1) clearly deems conformer **3** to be unfavorable, which was to be expected due to steric strain. Isomers **1** and **2** are close in energy, however the norbornadiene radical cation seemed to clearly favor the conformer in which the methyl group was oriented away from the phenyl ring (Figure 7, conformer **1**). All calculations with a starting geometry close to conformer **2** end with the geometry of **1**.

Based on these findings, the transition state and the influence of dispersion interactions were studied only for conformer **1** based on the B3LYP/6-311++G** level of theory with D3BJ dispersion correction. A more detailed look at the

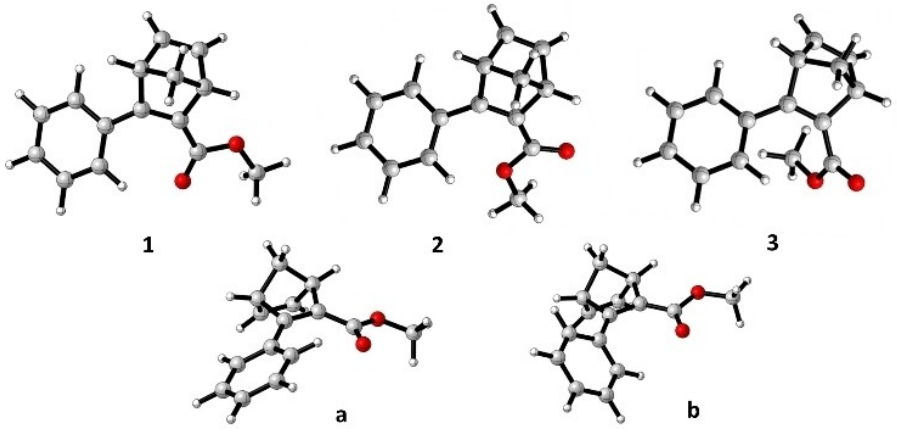

Figure 7. Optimized geometries of various possible conformers of the 2,3-disubstituted model compound.

Table 1. Comparison of relative energies of conformers **1–3** for each ground state in the isomerization mechanism. Energies calculated at the B3LYP/6-311++G** level of theory with D3BJ correction are given in kcal/mol.

	Conformer 1	Conformer 2	Conformer 3
NBD	0	0.4	8.7
QC	0	−0.8	10.1
NBD triplet	0	1.5	8.8
$NBD^{\bullet+}$	0	–	9.5
$QC^{\bullet+}$	0	1.1	14.9

results (Figure 6) in comparison with those of the unsubstituted core system shows a slight decrease in energy difference between the five of the six studied states. Only the quadricyclane ground state is higher in energy, causing a larger energy storage capacity. The energy barrier between the 2,3-disubstituted quadricyclane radical cation and the corresponding transition state however is even smaller than expected from the other results. The energy difference of around 1 kcal/mol lies in the range of conformer isomerization and is one possible explanation for the rapid back-conversion noticed in the experiments. The observed smaller energy differences go along with the experimental data for the similar substituted *push-pull* NBD derivative containing an ethyl ester functionality instead of the methyl substituent which was found to have an energy storage capacity of $\Delta H_{Storage} = 21.1$ kcal/mol, a value slightly lower than the 22 ± 1 kcal/mol measured for the unsubstituted system.[10b] Within the DFT investigations, we also simulated all three synthesized NBD-NDI hybrids **5 a-c**. Replacing the solubilizing heptyl chain by a methyl group, a substituent which barely impacts the rearrangement and storage capacity of the compounds, but drastically simplified the calculations. The effect of this adjustment was studied by calculations of the ground and radical anion states, showing ΔG^{298K} differences of only 0.2 kcal/mol. This small discrepancy can therefore be neglected in good conscience.

This model was then used to investigate possible intramolecular interactions within the synthesized NBD-NDI hybrids **5 a**–**c**. Optimized geometries of the ethyl-bridged compound **5 a** are shown in Figure 8, revealing the possibility of π-π-interactions between the phenyl substituent as well as the double bonds of NBD and the NDIs aromatic core. The comparison of the obtained ΔG^{298K} values of the NBD ground states (Table 2) shows that intramolecular interactions play a significant role, as the a significant role, as the open-chain conformer is the least favored isomer by 4.3 to 9.6 kcal/mol in all three compounds. The lowest energy conformation of both the ethyl- and butyl-linked hybrids includes π-π-interactions with the NBD double bond, whereas the longer bridging chain in **5 c** favors the stacking of the phenyl-substituent and the naphthalene core. This change can most likely be attributed to the decreasing steric strain once the bridging alkyl chain is long enough to make the stronger π-π-interaction between two aromatic structures possible. In all three cases the lowest energy NBD conformer led to the QC derivative with the highest relative energy. Another interesting observation was that the most stable conformer pair also lead to the highest energy storage capacity, as one can see in Table 2 where the QC energies are given relative to the NBD derivative in the same conformation.

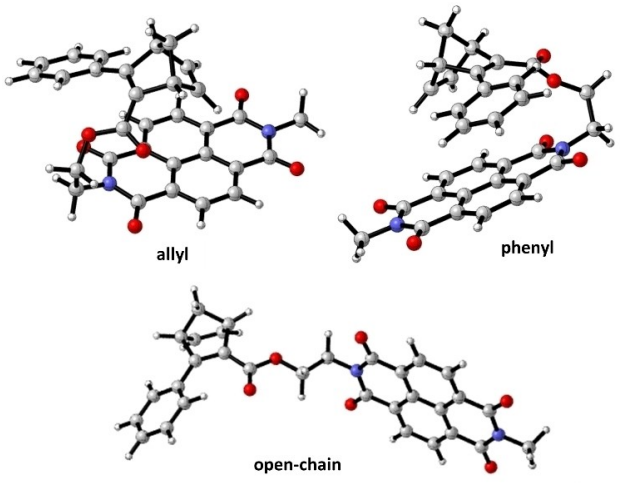

Figure 8. Optimized geometries of three possible conformers of compound **5 a**. The structures suggest π-π interactions between NBD double bonds and the aromatic NDI core ('allyl', top left), a π-stacking of phenyl substituent and NDI core ('phenyl', top right), or an open-chained structure (bottom).

Table 2. Comparison of relative energies of the three studied NBD-NDI hybrids with and without π-π interactions for the NBD and QC ground states. Energies calculated at the B3LYP/6-311++G** level of theory with D3BJ correction are given in kcal/mol. QC energies are given relative to their respective NBD conformer.

	Ethyl		Butyl		Hexyl	
	NBD	QC	NBD	QC	NBD	QC
Open-chain	4.3	26.2	4.4	26.2	9.6	26.1
Allyl	0	26.7	0	27.1	3.2	27.8
Phenyl	1.1	26.4	0.1	26.6	0	28.3

Conclusion

Three NBD-NDI hydride molecules were synthesized and characterized based on three also unprecedented naphthalene-diimide compounds with terminal hydroxy groups. Combining the photochromic norbornadiene and redox-active naphthalene diimide within one molecular architecture resulted in the formation of reversibly photoswitchable molecular architectures. The synthesized hybrids differ in the length of their spacer unit between the NBD and NDI building blocks and were investigated with respect to their photoisomerization behavior, the influence of the bridge length on this interconversion, and the concentration of the irradiated samples. Rearrangement of all hybrids to their corresponding QC derivatives takes place. The isomerization ratio to the corresponding QC derivative upon photoexcitation at 310 nm was determined by ^{1}H NMR spectroscopy and was found to plateau at 15–16.5% for all three compounds. The subsequent photoexcitation at 365 nm

caused in all three cases a rapid and clean back-conversion to the initial NBD-NDI structures. With increasing spacer length, a faster isomerization was observed during this reaction step. DFT calculations provided a viable explanation for these experimental results. With increasing spacer-length and the concomitant lowered steric strain, the π-π-interactions between the NBD and the NDI building block become more favorable. This leads to a facilitated intramolecular electron transfer and therefore a faster photo-oxidative conversion. An investigation of the concentration dependence revealed a reciprocal relationship between the concentration and the reaction rate. The higher the concentration of the irradiated sample was, the slower both steps of the isomerization were found to occur. This observation can so far only be explained by an increased collisional quenching of the NDI structures in more concentrated samples. The covalently linked hybrid molecules can be seen as a model for NBD/QC-dye photoswitches. Furthermore, rylene dyes were proven to have the potential to function as a photocatalyst for NBD/QC interconversion couples.

Experimental Section

All reagents and solvents were purchased from Sigma-Aldrich, Alfa Aesar or TCI and were used without further purification if not stated otherwise. The silica gel used in column chromatography was Kieselgel 60 M (deactivataed, 0.04–0.063 mm) purchased from Macherey-Nagel. Thin layer chromatography was performed on silica gel 60 F254 TLC-aluminium foils manufactured by Merck which were visualized by a UV lamp ($\lambda = 254$ and 365 nm). All NMR spectra were measured on a Bruker Avance 300 and an Avance 400 in various deuterated solvents which were used as purchased. Chemical shifts are given in ppm at room temperature and are referenced to residual protic impurities in the solvents (^{1}H: $CHCl_3$: 7.26 ppm) or the solvent itself ($^{13}C\{^1H\}$: $CDCl_3$: 77.16 ppm). The presented UV/vis absorption spectra were recorded on a Varian Cary 5000 UV-Vis-NIR spectrometer in DCM in quartz cuvettes ($d =$ 1 cm). Mass spectrometry (MALDI-TOF) was carried out on a AXIMA Confidence from Shimadzu Biotech, while high-resolution mass spectrometry (HRMS) was recorded on a maXis 4G from Bruker Daltonik.

NDI 4a: Compound **3** (150 mg, 0.411 mmol, 1.0 equiv.) and 2-aminoethanol (112 mg, 1.83 mmol, 4.5 equiv.) were dispersed in DMF (5 mL) and the mixture was heated to 130 °C for 1.5 h. After cooling to room temperature, the solvent was removed under reduced pressure and the crude product was purified by flash chromatography (SiO_2, DCM:EtOAc v:v 8:2, $R_f = 0.64$) and dried in vacuo. The product was isolated as a yellow solid (151 mg, 37.0 mmol, 90 %). **^{1}H NMR** ($CDCl_3$, 400 MHz) $\delta = 8.75$ (*d*, $J = 7.6$ Hz, 2 H), 8.72 (*d*, $J = 7.6$ Hz, 2 H), 5.25 (*m*, 1 H), 4.46 (*t*, $J = 5.6$ Hz, 2 H), 4.00 (*t*, $J = 5.2$ Hz, 2 H), 2.21–2.11 (*m*, 1 H), 1.95–1.84 (*m*, 1 H), 1.58 (*d*, $J =$ 6.8 Hz, 2 H), 1.37 - 1.18 (*m*, 6 H), 0.83 (*t*, $J = 6.8$ Hz, 3 H) ppm. **^{13}C NMR** ($CDCl_3$, 101 MHz) $\delta = 163.8$, 163.3, 131.3, 131.0, 127.4, 126.9, 126.8, 126.2, 61.3, 50.7, 43.1, 33.5, 31.7, 26.8, 22.6, 18.4, 14.1 ppm. **HRMS** (APPI, DCM) [M] m/z: 408.1680 (calc.), 408.1674 (found).

NDI 4b: Compound **3** (500 mg, 1.37 mmol, 1.0 equiv.) and 4-aminobutanol (296 mg, 3.94 mmol, 2.9 equiv.) were dissolved in DMF (10 ml) and the reaction mixture was heated to 130 °C for 1.5 h. After cooling to RT and removing of the solvent under reduced pressure, the crude product was purified by flash chromatography (SiO_2, EtOAc:DCM v:v 3:7, $R_f = 0.53$). Compound **4b** was isolated as a light-yellow solid (453 mg, 1.04 mmol, 76 %). **^{1}H NMR** ($CDCl_3$, 400 MHz) $\delta = 8.75$ (*d*, $J = 7.6$ Hz, 2 H), 8.73 (*d*, $J =$ 7.6 Hz, 2 H), 5.31–5.22 (*m*, 1 H), 4.26 (*t*, $J = 7.4$ Hz, 2 H), 3.74 (*q*, $J =$ 4.9 Hz, 2 H), 2.22–2.13 (*m*, 1 H), 1.96–1.82 (*m*, 3 H), 1.74–1.67 (*m*, 2 H), 1.58 (*d*, $J = 6.8$ Hz, 3 H), 1.48 (*t*, $J = 5.2$ Hz, 1 H), 1.38–1.19 (*m*, 6 H), 0.83 (*t*, $J = 6.4$ Hz, 3 H) ppm. **^{13}C NMR** ($CDCl_3$, 101 MHz) $\delta = 163.4$, 163.1, 131.1, 131.0, 127.3, 126.9, 126.7, 126.4, 62.5, 50.6, 40.6, 33.5, 31.7, 30.0, 26.8, 24.7, 22.6, 18.4, 14.1 ppm. **HRMS** (APPI, DCM/acetonitrile) $[M^+H^+]$ *m/z*: 437.2071 (calc.), 437.2079 (found).

NDI 4c: Compound **3** (150 mg, 0.411 mmol, 1.0 equiv.) and 6-aminohexanol (146 mg, 1.25 mmol, 3.0 equiv.) were suspended in DMF (5 mL) and heated to 130 °C for 1.5 h. Once cooled to room temperature, the solvent was removed under reduced pressure and the crude product was purified by flash chromatography (SiO_2, EtOAc:DCM v:v 3:7, $R_f = 0.56$). Compound **4c** was isolated as a beige solid (153 mg, 0.329 mmol, 80 %). **^{1}H NMR** ($CDCl_3$, 400 MHz) $\delta = 8.74$ (*d*, $J = 7.6$ Hz, 2 H), 8.72 (*d*, $J = 7.6$ Hz, 2 H), 5.30–5.21 (*m*, 1 H), 4.19 (*t*, $J = 7.6$ Hz, 2 H), 3.64 (*t*, $J = 6.4$ Hz, 2 H), 2.21–2.12 (*m*, 1 H), 1.95–1.86 (*m*, 1 H), 1.80–1.72 (*m*, 2 H), 1.63–1.57 (*m*, 5 H), 1.48–1.44 (*m*, 5 H), 1.37–1.18 (*m*, 6 H), 0.83 (*t*, $J = 6.8$ Hz, 3 H) ppm. **^{13}C NMR** ($CDCl_3$, 101 MHz) $\delta = 163.4$, 163.1, 131.1, 131.0, 127.2, 126.9, 126.7, 126.5, 62.9, 50.6, 40.9, 33.5, 32.7, 31.7, 28.1, 26.8, 25.4, 22.6, 18.4, 14.1 ppm. **HRMS** (APPI, DCM/acetonitrile) $[M^+H^+]$ *m/z*: 465.2384 (calc.), 465.2385 (found).

NBD-NDI 5a: Compound **4a** (132 mg, 0.324 mmol, 1.0 equiv.), compound **2** (138 mg, 0.651 mmol, 2.0 equiv.), DCC (144 mg, 0.647 mmol, 2.2 equiv.) and DMAP (15.2 mg, 0.124 mmol, 0.4 equiv.) were dissolved in dry DCM (20 mL) under argon atmosphere and refluxed for 6 h. The crude product was purified by column chromatography (DCM:THF v:v 99:1, $R_f = 0.26$) and recrystallized from acetonitrile. The product **5a** was obtained as a yellow solid (148 mg, 0.246 mmol, 76 %). **^{1}H NMR** ($CDCl_3$, 400 MHz) $\delta = 8.70$ (*d*, $J = 7.6$ Hz, 2 H), 8.66 (*d*, $J = 7.6$ Hz, 2 H), 7.36 (*d*, $J = 7.2$ Hz, 2 H), 7.08 (*t*, $J = 7.2$ Hz, 2 H), 7.13 (*t*, $J = 7.2$ Hz, 1 H), 6.91–6.89 (*m*, 1 H), 6.851–6.83 (*m*, 1 H), 5.32–5.23 (*m*, 1 H), 4.63–4.53 (*m*, 2 H), 4.48–4.39 (*m*, 2 H), 3.95 (*s*, 1 H), 3.76 (*s*, 1 H), 2.23–2.14 (*m*, 2 H), 2.00–1.89 (*m*, 2 H), 1.60 (*d*, $J = 6.8$ Hz, 3 H), 1.39–1.20 (*m*, 6 H), 0.85 (*t*, $J = 6.8$ Hz, 3 H) ppm. **^{13}C NMR** ($CDCl_3$, 101 MHz) $\delta = 167.6$, 165.0, 163.4, 162.9, 143.8, 140.5, 138.7, 135.3, 131.1, 130.9, 128.3, 127.8, 127.5, 127.2, 126.8, 126.7, 126.2, 70.3, 60.8, 58.5, 53.1, 50.6, 39.5, 33.6, 31.7, 26.9, 22.7, 18.4, 14.1 ppm. **HRMS** (APPI, DCM) $[M^+H^+]$ *m/z*: 603.2490 (calc.), 603.2486 (found).

NBD-NDI 5b: Compound **4b** (200 mg, 0.456 mmol, 1.0 equiv.), compound **2** (107 mg, 0.504 mmol, 1.1 equiv.), DCC (104 mg, 0.504 mmol, 1.1 equiv.) and DMAP (10 mg, 0.0820 mmol, 0.2 equiv.) were dissolved in dry DCM (20 mL) under argon atmosphere and refluxed for 4 h. After cooling to room temperature overnight, the solvent was removed and the crude product was purified by flash chromatography (DCM:hexane v:v 7:3 + 2 % THF). An additional column chromatography (DCM:THF v:v 99:1, $R_f = 0.39$) and recrystallization from acetonitrile gave the product as a yellow solid (65.7 mg, 0.104 mmol, 23 %). **^{1}H NMR** ($CDCl_3$, 400 MHz) $\delta = 8.75$ (*d*, $J = 7.6$ Hz, 2 H), 8.73 (*d*, $J = 7.6$ Hz, 2 H), 7.49–7.46 (*m*, 2 H), 7.34–7.29 (*m*, 2 H), 7.24–7.20 (*m*, 1 H), 6.99 - 6.97 (*m*, 1 H), 6.91 - 6.89 (*m*, 1 H), 5.31–5.22 (*m*, 1 H), 4.20–4.12 (*m*, 4 H), 4.06–4.05 (*m*, 1 H), 3.83–3.82 (*m*, 1 H), 2.26–2.23 (*m*, 1 H), 2.22–2.13 (*m*, 1 H), 2.06–2.04 (*m*, 1 H), 1.96–1.87 (*m*, 1 H), 1.77–1.68 (*m*, 4 H), 1.58 (*d*, $J = 6.8$ Hz, 3 H), 1.38–1.18 (*m*, 6 H), 0.83 (*t*, $J = 6.8$ Hz, 3 H) ppm. **^{13}C NMR** ($CDCl_3$, 101 MHz) $\delta = 167.0$, 165.6, 163.4, 163.0, 143.9, 141.0, 139.4, 135.9, 131.1, 131.0, 128.5, 127.9, 127.8, 127.2, 126.9, 126.7, 126.4, 70.7, 63.8, 58.7, 53.1, 50.6, 40.5, 33.5, 31.7, 26.8, 26.4, 24.9, 22.6, 18.4, 14.1 ppm. **HRMS** (APPI, DCM) $[M^+H^+]$ *m/z*: 631.2803 (calc.), 631.2807 (found).

NBD-NDI 5c: Compound **4c** (125 mg; 0.269 mmol; 1.0 equiv.), compound **2** (122 mg, 0.575 mmol, 2.1 equiv.), DCC (119 mg,

0.577 mmol, 2.1 equiv.) and DMAP (12.0 mg, 0.0982 mmol, 0.4 equiv.) were dissolved in dry DCM (15 ml) under argon atmosphere and refluxed for 4 h. The sample was allowed to cool to room temperature overnight, before the solvent was removed under reduced pressure. The crude product was purified by column chromatography (DCM:THF v:v 99:1, $R_f = 0.33$) and recrystallized from acetonitrile. Compound **5c** was obtained as a yellow solid (125 mg, 190 mmol, 71%). **^{1}H NMR** ($CDCl_3$, 400 MHz) $\delta = 8.75$ (*d*, $J =$ 7.6 Hz, 2 H), 8.73 (*d*, $J = 7.6$ Hz, 2 H), 7.50–7.47 (*m*, 2 H), 7.36–7.27 (*m*, 2 H), 6.99–6.97 (*m*, 1 H), 6.92–6.90 (*m*, 1 H), 5.31–5.22 (*m*, 1 H), 4.18 (*t*, $J = 7.5$ Hz, 2 H), 4.11–4.02 (*m*, 4 H), 2.26–2.24 (*m*, 1 H), 2.22–2.13 (*m*, 1 H), 2.06–2.04 (*m*, 1 H), 1.97–1.83 (*m*, 1 H), 1.71 (*m*, 2 H), 1.63–1.56 (*m*, 5 H), 1.44–1.19 (*m*, 10 H), 0.83 (*t*, $J = 6.8$ Hz, 3 H) ppm. **^{13}C NMR** ($CDCl_3$, 101 MHz) $\delta = 166.7$, 165.7, 163.4, 163.0, 143.9, 141.3, 141.0, 139.5, 136.0, 131.1, 131.0, 128.8, 128.6, 127.9, 126.9, 126.7, 126.5, 126.1, 70.7, 64.3, 58.7, 53.1, 50.6, 40.9, 33.5, 31.7, 29.8, 28.6, 28.1, 26.8, 26.8, 25.9, 22.6, 18.4, 14.1 ppm. **HRMS** (APPI, DCM) $[M^+H^+]$ $m/z = 659.3116$ (calc.), 659.3121 (found).

Acknowledgements

A.L. and C.W. contributed equally to this work. We gratefully thank the German Research Council (DFG) for funding through project 391585168 "Photochemisch und magnetochemisch ausgelöste Speicherung/Freisetzung von Sonnenergie in gespannten organischen Verbindungen". Additionally, we would like to thank the Bavarian Collaborative Research Project Solar Technologies go Hybrid (SolTech), the Cluster of Excellence "Engineering of Advanced Materials" (EAM), funded by DFG, the Graduate School Molecular Science (GSMS) and the Graduate School Advanced Materials and Processes (GSAMP) for financial support. Open Access funding enabled and organized by Projekt DEAL.

Conflict of Interest

The authors declare no conflict of interest.

Data Availability Statement

The data that support the findings of this study are available from the corresponding author upon reasonable request.

Keywords: energy conversion · molecular photoswitches · naphthalene diimide · norbornadiene · quadricyclane

[1] a) S. Vazquez, S. Lukic, E. Galvan, L. G. Franquelo, J. M. Carrasco, J. I. Leon, in *IECON 2011–37th Annual Conference of the IEEE Industrial Electronics Society* **2011**, pp. 4636–4640; b) A. K. Sharma, C. Sharma, S. C. Mullick, T. C. Kandpal, *Renewable Sustainable Energy Rev.* **2017**, *78*, 124–137; c) D. Gielen, F. Boshell, D. Saygin, M. D. Bazilian, N. Wagner, R. Gorini, *Energy Strategy Rev.* **2019**, *24*, 38–50; d) P. Preuster, C. Papp, P. Wasserscheid, *Acc. Chem. Res.* **2017**, *50*, 74–85; e) A. Lennartson, K. Moth-Poulsen, in *Molecular Devices for Solar Energy Conversion and Storage* (Eds.: H. Tian, G. Boschloo, A. Hagfeldt), Springer Singapore, Singapore, **2018**, pp. 327–352.
[2] a) G. S. Hammond, P. Wyatt, C. D. DeBoer, N. J. Turro, *J. Am. Chem. Soc.* **1964**, *86*, 2532–2533; b) Z. Wang, A. Roffey, R. Losantos, A. Lennartson, M. Jevric, A. U. Petersen, M. Quant, A. Dreos, X. Wen, D. Sampedro, K. Börjesson, K. Moth-Poulsen, *Energy Environ. Sci.* **2019**, *12*, 187–193.
[3] F. Waidhas, M. Jevric, L. Fromm, M. Bertram, A. Görling, K. Moth-Poulsen, O. Brummel, J. Libuda, *Nano Energy* **2019**, *63*, 103872.
[4] a) Y. Harel, A. W. Adamson, C. Kutal, P. A. Grutsch, K. Yasufuku, *J. Phys. Chem.* **1987**, *91*, 901–904; b) W. L. Dilling, *Chem. Rev.* **1966**, *66*, 373–393.
[5] a) M. Quant, A. Lennartson, A. Dreos, M. Kuisma, P. Erhart, K. Börjesson, K. Moth-Poulsen, *Chem. Eur. J.* **2016**, *22*, 13265–13274; b) V. Gray, A. Lennartson, P. Ratanalert, K. Börjesson, K. Moth-Poulsen, *Chem. Commun.* **2014**, *50*, 5330–5332.
[6] X.-w. An, Y.-d. Xie, *Thermochim. Acta* **1993**, *220*, 17–25.
[7] R. B. Woodward, R. Hoffmann, *Angew. Chem. Int. Ed. Engl.* **1969**, *8*, 781–853.
[8] a) H. Frey, *J. Chem. Soc.* **1964**, 365–367; b) C. Qin, Z. Zhao, S. R. Davis, *J. Mol. Struct.: THEOCHEM* **2005**, *728*, 67–70.
[9] a) T. B. Patrick, D. S. Bechtold, *J. Org. Chem.* **1984**, *49*, 1935–1937; b) G. Jones, S.-H. Chiang, W. G. Becker, D. P. Greenberg, *J. Chem. Soc. Chem. Commun.* **1980**, 681–683.
[10] a) P. Lorenz, A. Hirsch, *Chem. Eur. J.* **2020**, *26*, 5220–5230; b) T. Luchs, P. Lorenz, A. Hirsch, *ChemPhotoChem* **2020**, *4*, 52–58.
[11] P. Lorenz, T. Luchs, A. Hirsch, *Chem. Eur. J.* **2021**, *27*, 4993–5002.
[12] E. Haselbach, T. Bally, Z. Lanyiova, P. Baertschi, *Helv. Chim. Acta* **1979**, *62*, 583–592.
[13] R. W. Hoffmann, W. Barth, *J. Chem. Soc. Chem. Commun.* **1983**, *7*, 345–346.
[14] a) K. Ishiguro, I. V. Khudyakov, P. F. McGarry, N. J. Turro, H. D. Roth, *J. Am. Chem. Soc.* **1994**, *116*, 6933–6934; b) H. D. Roth, M. L. M. Schilling, G. Jones, *J. Am. Chem. Soc.* **1981**, *103*, 1246–1248.
[15] M. Yasuda, R. Kojima, H. Tsutsui, D. Utsunomiya, K. Ishii, K. Jinnouchi, T. Shiragami, T. Yamashita, *J. Org. Chem.* **2003**, *68*, 7618–7624.
[16] a) S. Alp, Ş. Erten, C. Karapire, B. Köz, A. O. Doroshenko, S. İçli, *J. Photochem. Photobiol. A* **2000**, *135*, 103–110; b) G. Jones, S. H. Chiang, W. G. Becker, J. A. Welch, *J. Phys. Chem.* **1982**, *86*, 2805–2808.
[17] a) S. Guha, F. S. Goodson, S. Roy, L. J. Corson, C. A. Gravenmier, S. Saha, *J. Am. Chem. Soc.* **2011**, *133*, 15256–15259; b) S. V. Bhosale, C. H. Jani, S. J. Langford, *Chem. Soc. Rev.* **2008**, *37*, 331–342.
[18] S. Caby, L. M. Bouchet, J. E. Argüello, R. A. Rossi, J. I. Bardagi, *ChemCatChem* **2021**, *13*, 3001–3009.
[19] M. Fujitsuka, S. S. Kim, C. Lu, S. Tojo, T. Majima, *J. Phys. Chem. B* **2015**, *119*, 7275–7282.
[20] G. Andric, J. F. Boas, A. M. Bond, G. D. Fallon, K. P. Ghiggino, C. F. Hogan, J. A. Hutchison, M. A.-P. Lee, S. J. Langford, J. R. Pilbrow, *Aust. J. Chem.* **2004**, *57*, 1011–1019.
[21] a) T. W. Kim, S. H. Kim, J. W. Shim, D. K. Hwang, *Front. Optoelectron.* **2022**, *15*, 1–7; b) Y. Wakayama, R. Hayakawa, K. Higashiguchi, K. Matsuda, *J. Mater. Chem. C* **2020**, *8*, 10956–10974; c) A. Dreos, Z. Wang, B. E. Tebikachew, K. Moth-Poulsen, J. Andréasson, *J. Phys. Chem. Lett.* **2018**, *9*, 6174–6178.
[22] a) A. D. Dubonosov, V. A. Bren, V. A. Chernoivanov, *Russ. Chem. Rev.* **2002**, *71*, 917–927; b) G. K. Tranmer, W. Tam, *J. Org. Chem.* **2001**, *66*, 5113–5123.
[23] A. R. Tuktarov, A. R. Akhmetov, A. A. Khuzin, U. M. Dzhemilev, *J. Org. Chem.* **2018**, *83*, 4160–4166.
[24] A. A. Berezin, A. Sciutto, N. Demitri, D. Bonifazi, *Org. Lett.* **2015**, *17*, 1870–1873.
[25] R. D. Bach, I. L. Schilke, H. B. Schlegel, *J. Org. Chem.* **1996**, *61*, 4845–4847.

Manuscript received: May 10, 2022
Accepted manuscript online: July 1, 2022
Version of record online: August 1, 2022